Predicting propagation from a point source over grooved ground using a modal model

Steve Mellish, Shahram Taherzadeh, Keith Attenborough

PREDICTING PROPAGATION FROM A POINT SOURCE OVER GROOVED GROUND USING A MODAL MODEL

Steve Mellish **Shahram Taherzadeh** **Keith Attenborough**
Faculty of STEM, The Open University, UK
steve@melectronics.co.uk

ABSTRACT

A modal model, hitherto used to predict electromagnetic and ultrasonic surface waves, is employed in deriving an effective impedance for a grooved acoustically hard surface. This is inserted in the classical theory for propagation from a point source above an impedance plane to predict point-to-point propagation above regularly spaced grooves with rectangular cross sections. Predictions of excess attenuation (EA) spectra obtained in this manner compare closely with those obtained by a numerical method (BEM) but take a fraction of the time. The modal method is extended to predict EA spectra above metasurfaces consisting of repeated arrays of variable depth grooves with different depths of a low flow resistivity porous material in each groove. The porous infill is predicted to reduce the negative EA peaks associated with quarter wavelength resonances in the grooves. By applying the modal model effective impedance theory, porous-infill groove arrays have been designed to yield wideband excess attenuation spectra with potential for reducing noise from surface transport.

1. INTRODUCTION

Outdoor propagation of sound from a point or line source over a rough ground where the incident wavelengths are larger than or comparable with the dimensions of the roughness involves both scattering and coherent reflection. The coherent component of the ground reflection interferes constructively and destructively with sound travelling directly from source to receiver. Many theories have been published to predict the scattering behaviour of particular forms of periodic structure beginning with Rayleigh for sinusoidal surfaces [22] and latterly those such as multiple scattering or boss theory [23, 31, 32] and modal decompositions [1–3, 19, 24–26, 28] which solve for the scattered field. Recently there has been interest in deliberately profiling the ground surface in a periodic manner to cause destructive interference in a frequency range useful for reducing noise from surface transport sources [14, 21, 30].

Propagation over such surfaces can be predicted by numerical methods such as the Boundary Element Method (BEM) in the frequency domain and by Finite Difference Time Domain and Pseudo-Spectral Time Domain. However, these methods are rather computationally demanding. The computational demands can be reduced significantly if the rough surface can be represented by an effective impedance plane rather than having to input the detail of the surface topography. This has been done empirically for a surface composed from regularly spaced low parallel walls based on laboratory measurements [30]. But computational requirements are reduced even further, and the effective impedance approach made more general if the effective impedance can be expressed analytically, since this can be used in a classical theory for predicting point-to-point propagation over an impedance plane [17, 18, 20, 27]. This paper uses a modal method adapted from electromagnetic theory [1] to derive an effective impedance near grazing incidence. A classical theory for point-to-point propagation is outlined in section 2. The modal model for the total field above a periodic system of variable depth grooves incorporating porous layers is described briefly in Section 3 along with the derivation of a corresponding effective impedance. Section 4 presents predictions of excess attenuation spectra for source and receiver at 0.1 m height and separated by 2 m above three types of periodic surfaces involving rectangular grooves, identical acoustically-hard grooves, grooves with different depths intended to introduce a phase gradient during reflection and a 'metasurface' composed from grooves with different depths containing different thicknesses of a rigid-porous material. Excess attenuation spectra calculated using the modal model's effective impedance are shown to compare favourably with those obtained using the more computationally expensive BEM and the 'metasurface' is predicted to result in a broad band attenuation.

2. POINT-TO-POINT ACOUSTIC PROPAGATION ABOVE A GROUND PLANE

Many outdoor acoustics problems involving transport noise may be modelled as a point source and receiver in space, above a ground plane of the form shown in Fig. 1. Where one wishes to calculate the magnitude of the sound reaching the receiver, usually a populated area, from a nuisance noise source such as a road, industrial facility or airport. The intervening ground is modelled as an effective impedance [14, 17, 18] and the sound reaching the receiver is the addition of the component directly from the source along path R_i and that specularly reflected from the homogeneous ground surface following the path $R_B + R_A$. The sound from the source incident upon the ground with angle θ will be reflected by a factor given by a reflection coefficient Γ, which may be chosen to suit each application and is a function of the effective impedance of the

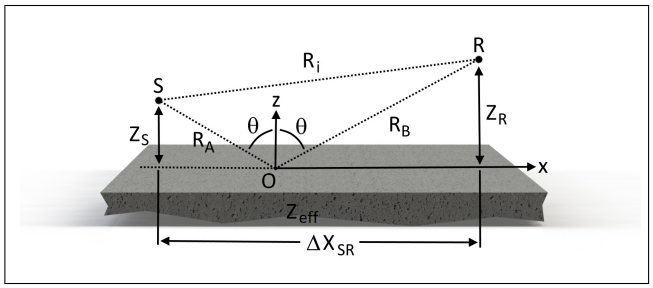

Figure 1. Point-to-point acoustic propagation model.

ground surface Z_{eff}. For this study the reflection coefficient of Chien and Soroka [12] for a spherical spreading source and denoted Γ_S will be used. The generally applied method of expressing the results is in the form of excess-attenuation (EA) as shown in (1) for spherical spreading. It is a measure of the effect of the ground surface relative to a given reference, such as the free-field or another reference ground surface. This allows noise attenuating ground surfaces to be objectively evaluated relative to a control surface.

$$EA_{dB} = 20\log\left(\left|1+\frac{\Gamma_S \exp\left(ik\left(R_A+R_B\right)\right)/\left(4\pi\left(R_A+R_B\right)\right)}{\exp\left(ikR_i\right)/\left(4\pi R_i\right)}\right|\right) \quad (1)$$

The point-to-point model of Fig. 1 assumes that the ground is homogeneous and reflection is purely specular given by the combination of the incident 'i' and ground reflected 'r' components thus,

$$p_{tot}(x_R, z_R) = p_i + p_r \quad (2)$$

However, in the presence of a scattering ground surface where the features are comparable in size to the incident wavelength, such as those under consideration in this work, an additional scattered 'sct' component is present and so the field at the receiver becomes,

$$p_{tot}(x_R, z_R) = p_i + p_r + p_{sct} \quad (3)$$

A method for efficiently determining an approximation to the scattered field and incorporating this into Z_{eff} follows henceforth.

3. DERIVING AN EFFECTIVE IMPEDANCE FOR RECTANGULARLY GROOVED SURFACES

3.1 A modal model for singularly grooved periodic surfaces

A solution to the problem of calculating the electromagnetic field above a perfectly reflecting rectangular grooved periodic surface structure, as defined by the pitch d, aperture a and depth h as in Fig. 2, was presented by Hessel *etal*. [1] and laterly applied by Kelders *etal*. [2, 3] to acoustics to study the ultrasonic surface waves supported by such structures. The method has recently been extended by the authors [4] to approximate the grooved surface as an effective ground plane impedance to allow point-to-point acoustic propagation problems involving these structures to be efficiently modelled. In order to apply the point-to-

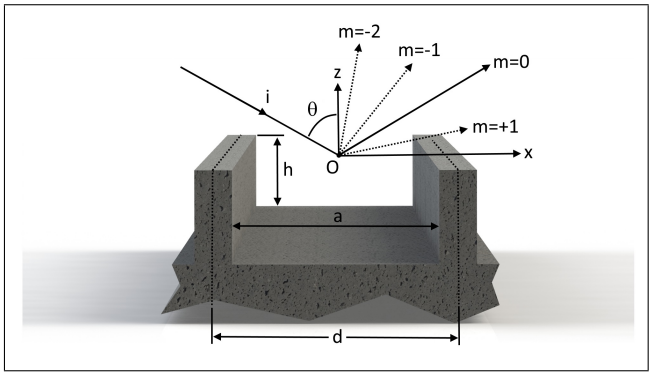

Figure 2. Rectangular groove definition and resulting scattered field.

point model of Fig. 1 to a rectangularly grooved surface, it is required that the surface be represented as an approximate impedance which in turn, necessitates the solution of the scattered field, for which the modal model will be employed.

The modal model relies upon the simplifying assumptions that the grooved surface is acoustically hard and extends infinitely in all horizontal dimensions which for the 2-dimensional case with which this paper in concerned, leads to infinite spatial periodicity in the x-axis (see Fig. 2) and spatial invariance in y. Excitation is by homogeneous plane wave within an ideal inviscid medium, with a given angle of incidence θ and propagation constant k in the x-z plane. A brief appraisal of the modal model kernel is given here with an assumed $\exp(-i\omega t)$ time convention, but reference is made to literature for a comprehensive derivation [1–4].

The domain of the 2d problem may be considered as two separate half spaces within the x-z plane, the free field upper space for $z > 0$ and the lower groove space where $z < 0$. Both spaces exhibit infinite periodicity in x owing to the infinite extents of the periodic grooved structure combined with homogenous plane wave excitation. This constrains the propagation characteristics of each half space region to that of an infinite set of m and n discrete modes for the upper and lower half spaces respectively, with complex amplitudes weightings of $\hat{V_m}$ (upper space quantities are denoted by hat) and V_n. Where the $\hat{V_m}$ and V_n sets are mutually related by the inner product relationships of,

$$\begin{aligned} \hat{V_m} &= \sum_n V_n \langle e_n, *\hat{e_m} \rangle \\ V_n &= \sum_m \hat{V_m} \langle e_n, \hat{e_m} \rangle \end{aligned} \quad (4)$$

Where $\hat{V_0} = \hat{V_0^i} + \hat{V_0^r}$ and the incident wave amplitude $\hat{V_0^i}$ is given as initial conditions of the problem and most conveniently given the value of 1. As the problem is posed in terms of z-direction velocity v_z and acoustic pressure p, then impedance relationships which relate the acoustic pressure to v_z for each free-space mode m, is as below and

Z_c is the characteristic impedance of the ideal inviscid air medium.

$$\begin{aligned} \hat{Z_m} &= \frac{Z_c k}{\hat{k_m^z}} \\ \hat{Z_m^i} &= -\hat{Z_m^r} = -\hat{Z_0} \end{aligned} \tag{5}$$

where the z-axis propagation constant $\hat{k_m^z}$ for the free-space mode m given by,

$$\hat{k_m^z} = \sqrt{k^2 - \left(k \sin\theta + \frac{2m\pi}{d}\right)^2} \tag{6}$$

The propagation geometry of the free-field modes are given solely by θ and the periodicity of the grating d with the mode function e_m for each discrete mode m being defined on $z = 0$ as,

$$\hat{e_m} = d^{-0.5} \exp\left(i\left[k \sin\theta + \frac{2m\pi}{d}\right] x\right) \tag{7}$$

Each groove is assumed to behave as an acoustically hard walled and bottomed waveguide which defines the modes which may exist within it and the modal characteristics that this will present at the aperture of each groove at $z = 0$. This is dependent upon the groove aperture a and given by the mode function e_n within the extents of the groove aperture $|x| \leq a/2$ at $z = 0$.

$$\begin{aligned} e_{n>0} &= \sqrt{\frac{2}{a}} \cos\left(\left[\frac{n\pi}{a}\right]\left[x + \frac{a}{2}\right]\right) \\ e_0 &= \sqrt{\frac{1}{a}} \cos\left(\left[\frac{n\pi}{a}\right]\left[x + \frac{a}{2}\right]\right) \end{aligned} \tag{8}$$

With each n mode possessing the z-axis propagation constant k_n^z within the groove of,

$$k_n^z = \pm\sqrt{k^2 - \left(\frac{n\pi}{a}\right)^2} \tag{9}$$

The impedance at the aperture of the groove Z_n, due to the combination of the incident and reflected component from the bottom of the groove is given by the well known relationship,

$$Z_n = -i\frac{Z_c k}{k_n^z} \cot\left(k_n^z h\right) \tag{10}$$

The modal model solution is obtained by truncating n to N and m to $\pm M$ equating the two mode systems in terms of vertical velocity v_z at their boundary $z = 0$ and solving the following system of $N \times N$ equations to yield the set of V_n modal amplitudes for the groove space.

$$\begin{aligned} \sum_{n\dagger} V_{n\dagger} \left(\sum_m \left[\hat{Z_m} \langle e_{n\dagger}, *\hat{e}_m\rangle \langle e_n, \hat{e}_m\rangle\right] - \delta_n^{n\dagger} Z_n\right) \\ = -2\hat{Z_0^i}\hat{V_0^i}\langle e_n, \hat{e}_0\rangle \end{aligned} \tag{11}$$

Expanding (3), the homogenous plane wave pressure field p_{tot} is therefore given by the summation of all modes thus,

$$\begin{aligned} p_{tot}(x_R, z_R) =& \hat{Z_0^i}\hat{V_0^i}\hat{e_0} \exp\left(-i\hat{k_0^z} z\right) \\ &+ \hat{Z_0^r}\hat{V_0^r}\hat{e_0} \exp\left(i\hat{k_0^z} z\right) \\ &+ \sum_{m\neq 0} \hat{Z_m}\hat{V_m}\hat{e_m} \exp\left(ik_m^z z\right) \end{aligned} \tag{12}$$

3.2 Multiple groove periodic surfaces with porous layers

The modal model is extended for structures with multiple grooves within each period, having individual dimensions and a porous layer of depth l occupying the lower portion of each groove, as shown in Fig. 3. Such structures are frequently termed in recent literature as metasurfaces or phase gradient structures [5–11]. The model is similar to that of single groove but the parameters become 2-dimensional with the addition of the index q, relating to the q'th groove within each period from $q = 0$ to $q = K$ where $K + 1$ is the number of grooves per grating period d. As the geometry of the scattered field depends only upon the pitch of the grating structure, d in Fig. 3, then the definitions for the free-space modal field of (5) (6) (7) remain unchanged save for the addition of the index q.

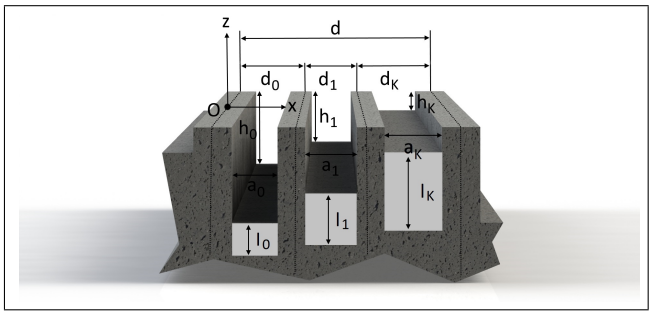

Figure 3. Multiple grooved periodic surface with porous layers.

The v_z boundary condition of the groove space at $z = 0$, however, is more complex, becoming the concatenation of all $K + 1$ groove elements as in (13).

$$\begin{aligned} v_z(x,0) = &\left[\sum_{n=0}^{N} V_{0,n} e_{0,n}\right]_{x=0}^{x=d_0} \parallel \\ &\left[\sum_{n=0}^{N} V_{1,n} e_{1,n}\right]_{x=d_0}^{x=d_0+d_1} \parallel \ldots \\ &\left[\sum_{n=0}^{N} V_{K,n} e_{K,n}\right]_{x=d_0+d_1+\ldots d_{K-1}}^{x=d} \end{aligned} \tag{13}$$

To ensure continuity, each $e_{q,n}$ mode function will have x-extents from 0 to d with a zero value outside of the aperture a_q. Within the aperture a_q, the function will be that of (8), retaining the same normalisation to aperture width a_q, due to the length padding to d being zero valued. The definition of $e_{q,n}$ for the multiple featured grating, evaluated in the

region $x = 0$ to $x = d$, becomes,

$$
\begin{aligned}
e_{q,n>0} = & \\
& \delta_e \sqrt{\frac{2}{a_q}} \cos\left(\left[\frac{n\pi}{a_q}\right]\left[x - \sum_{j<q} d_j + \frac{d_q - a_q}{2}\right]\right) \\
e_{q,0} = & \delta_e \sqrt{\frac{1}{a_q}} \\
\delta_e = & \begin{bmatrix} 1 & x \geq \sum_{j<q} d_j + \frac{d_q - a_q}{2} \\ 1 & x \leq \sum_{j \leq q} d_j - \frac{d_q - a_q}{2} \\ 0 & else \end{bmatrix} j \in \mathbf{Z}^+
\end{aligned}
\tag{14}
$$

The resulting system of equations, which is solved numerically as a K $(N \times N)$ matrix, becomes,

$$
\begin{aligned}
& \sum_{q\dagger} \sum_{n\dagger} V_{q\dagger,n\dagger} \\
& \qquad \left(\sum_m \left[\hat{Z_m} \langle e_{q\dagger,n\dagger}, *\hat{e}_m \rangle \langle e_{q,n}, \hat{e}_m \rangle \right] - \delta_{q,n}^{q\dagger,n\dagger} Z_{q,n} \right) \\
& \qquad = -2\hat{Z_0^i}\hat{V_0^i} \langle e_{q,n}, \hat{e}_0 \rangle \\
& \delta_{q,n}^{q\dagger,n\dagger} = \begin{bmatrix} 1 & a = a\dagger, q = q\dagger \\ 0 & else \end{bmatrix}
\end{aligned}
\tag{15}
$$

Adding a porous element to the lower portion of each groove will alter the impedance at the aperture and hence may be implemented by modifying only the $Z_{q,n}$ term in (15), leaving the rest of the model unchanged. The impedance at the groove aperture will be given by the combination of the incident wave and that reflected from the air/porous material boundary at $z = -h_q$, which in turn depends upon the impedance that the porous layer presents, Z_L, at the boundary. The reflection coefficient at the boundary is given by (16), where the usual angle of incidence dependence is omitted because the system of equations for this model are already posed in terms of the surface normal v_z.

$$
\gamma = -\frac{1 - (1/Z_L(q,n))}{1 + (1/Z_L(q,n))} \tag{16}
$$

The surface impedance Z_L at $z = -h_q$, is calculated using an appropriate effective impedance model for a hard-backed porous layer [14, 15, 17, 18] while being mindful of the corresponding assertions the chosen model makes about the physical properties of the material. If a locally reacting model is chosen all propagation within the layer is assumed to be plane-wave and perpendicular to the surface, so Z_L will not be dependent upon the angle with which the groove mode is incident upon the air/porous material boundary θ_n. Non-locally reacting impedance models able to support transverse modes will have a dependence upon θ_n, thus Z_L will be a function of θ_n. The resultant impedance across the aperture for the q'th groove and mode n posed in terms of v_z, is given by the interaction of the down-going and reflected up-going modal components within the groove thus,

$$
Z_{q,n} = \frac{Z_c k}{k_{q,n}} \frac{(-1 + \gamma \exp(ik_{q,n} 2h_q))}{1 + \gamma \exp(ik_{q,n} 2h_q)} \tag{17}
$$

Using (14)(16)(17) and the unaltered equations of 3.1 in (15), then solving numerically the resulting matrix, yields the solution of the plane wave field above the multiple featured grooved surface of Fig. 3. For the case of a single groove ($K = 0$) and a zero porous layer depth, the multiple (3.2) and single grooved (3.1) models are equivalent.

3.3 Deriving an effective impedance from the homogeneous modal model field

In this section the modal model solution to the homogeneous plane wave field will be used to deduce an effective impedance Z_{eff} for the periodically grooved surface. This approach is advantageous over simply taking the plane wave field directly, which is not appropriate for fields involving line or point source excitation. Firstly, Z_{eff} is approximately wave type independent allowing direct application to the point-to-point model with a line or point source. Furthermore, the plane wave summation does not generally exhibit a surface wave, but it is implicit in Z_{eff} as a property of the surface itself, so will be apparent upon application to a spherical or cylindrical reflection coefficient Γ_S [12, 16].

The plane wave field at the (x, z) receiver location R, defined in Fig. 1, is given by the accumulation of the free-space modes as in (12). To improve similarity with practical outdoor acoustic problems, a geometric scheme is introduced [4] to limit the extent of the grooved surface to between the points x_1 and x_2 defined in Fig. 4. Modes which

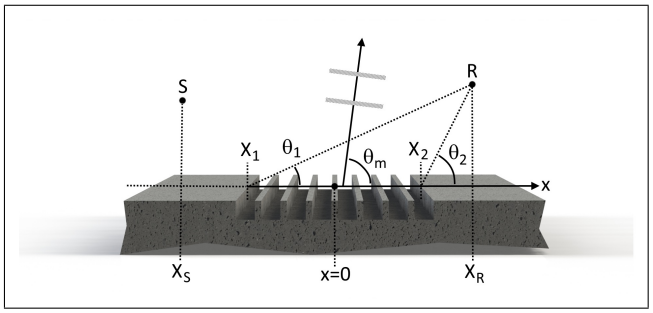

Figure 4. Rectangular groove definition and resulting scattered field.

would not geometrically intersect the receiver are omitted form the summation of (12). Evanescent modes possessing an imaginary k_m^z are also omitted because they are surface modes present only to solve the boundary conditions in the presence of the homogeneous incident plane wave, not a true surface wave [19]. With reference to Fig. 4, this is achieved by defining the following Kronecker delta funciton thus,

$$
\delta_{\theta_2}^{\theta_1}(\theta_m) = \begin{bmatrix} 1 & \theta_2 \geq \theta_m \geq \theta_1 \\ 0 & \Im(\theta_m) > 0 \\ 0 & else \end{bmatrix} \tag{18}
$$

Applying this to (12) to ensure that modes which do not satisfy (18) are not included in the field, leads to the revised field summation of,

$$\begin{aligned} p_{tot}(x_R, z_R) =& \hat{Z_0^i}\hat{V_0^i}\hat{e_0}\exp\left(-i\hat{k_0^z}z\right) \\ &+\hat{Z_0^r}\hat{V_0^r}\hat{e_0}\exp\left(i\hat{k_0^z}z\right) \\ &+\sum_{m\neq 0}\delta_{\theta_2}^{\theta_1}(\theta_m)\hat{Z_m}\hat{V_m}\hat{e_m}\exp\left(i\hat{k_m^z}z\right) \end{aligned} \tag{19}$$

Although x_1 and x_2 may be set arbitrarily, they will be assumed henceforth to coincide horizontally with x_S and x_R respectively so that the grating structure occupies the space between the source and receiver.

From the field at point R and including a phase constant to remove the plane wave path length difference between the incident and reflected components l_{PD}, the plane wave reflection coefficient Γ_P of the grooved surface may be calculated as follows,

$$\Gamma_P = \frac{p_r(x_R, z_R) + p_{sct}(x_R, z_R)}{p_i(x_R, z_R)\exp\left(-ikl_{PD}\right)} \tag{20}$$

Rearranging (20) to the form of (21), yields the effective impedance for the grooved surface, Z_{eff}.

$$Z_{eff} = \frac{(1+\Gamma_P)\sec\theta}{1-\Gamma_P} \tag{21}$$

The grooved surface is now represented by an equivalent impedance which is locally reacting, valid only for the angle of incidence θ for which it was calculated.

4. RESULTS

Predictions from the modal model are compared with those from a Boundary Element Method (BEM). The impedance of the porous layer Z_L, will be represented by the slit-pore impedance model [17] as it has been shown to give good agreement with a variety of typical outdoor ground surface types [14]. A porosity of 0.5 and flow resistivity of 5.43×10^3 will be applied which is typical of a suitable gravel filling for the size of grooves in question. Predictions of Excess-attenuation spectra, referenced to the free-field, are presented in the frequency band 100 to $2000Hz$, where much man-made nuisance noise is focused [14, 21]. In line with existing work [1, 2, 4], truncations of $N = 5$ and $M = 25$ are used within the modal model. The process of obtaining the results from the modal model is to numerically solve the system of equations (15), accumulate the plane wave field using (19), then from this calculate Z_{eff} with (21) and calculate the EA spectrum using (1).

Three results are shown, a single grooved grating in Fig. 5, a periodic structure in which each period contains three hard bottomed grooves of different depths and no porous layer in Fig. 6 and the same but with a porous layer in each of the three grooves in Fig. 7. For ease of comparison Fig. 8 shows the three modal plots overlaid.

It is apparent that the extended modal model agrees well with the BEM predictions but with a significantly shorter computation time, approximately 2 hours for Fig. 6 with BEM versus a few minutes for the modal result.

The multiple destructive interference minima of Fig. 6 are evident due to the multiple depth grooves whereas just a single such minimum is observed in Fig. 5 for the single groove. Adding the porous layer then flattens the response to a wide band attenuation of the noise level in Fig. 7. This characteristic is desirable for noise attenuating structres and future work will attempt to lower the frequency at which this attenuation occurs to further improve the practical applicability. Addition of the porous layer also reduces the magnitude of the surface wave which will in part be due to losses of the porous layer. However the slope around the first minimum is shallowed and attenuation in this region is less than for the non-porous layered structures.

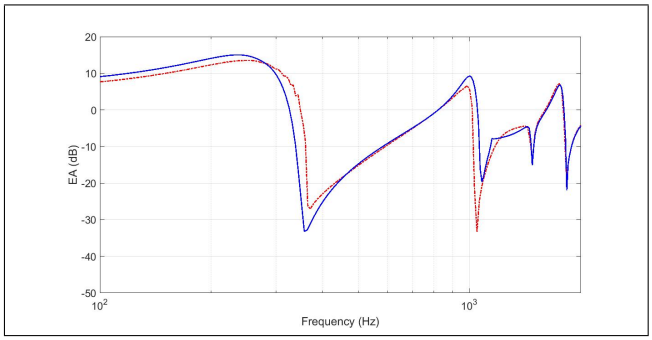

Figure 5. Single rectangular groove, d=0.15, a=0.12, h=0.2 (Solid=Modal (Z_{eff}), broken=BEM).

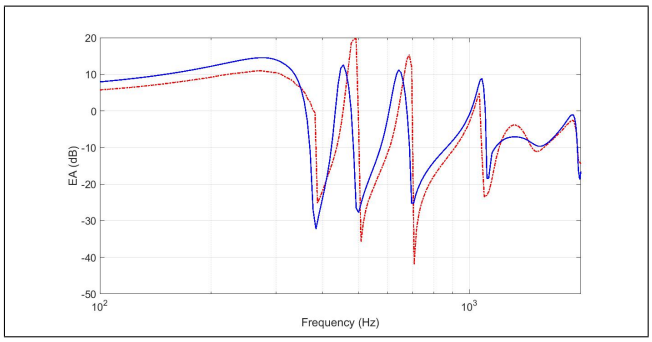

Figure 6. Three hard bottomed rectangular grooves per period without porous layer, d_q=[0.05,0.05,0.05], a_q=[0.04,0.04,0.04], h_q=[0.2, 0.15, 0.1] (Solid=Modal (Z_{eff}), broken=BEM).

5. CONCLUSIONS

Predicting the noise attenuating properties of rectangularly grooved structures has traditionally been computationally expensive. An efficient modal model has been extended and successfully applied to obtain an effective impedance for complex rectangularly grooved ground surfaces. This has shown good agreement with BEM for excess-attenuation spectra for point to point acoustic propagation, but with a significantly lower computation time.

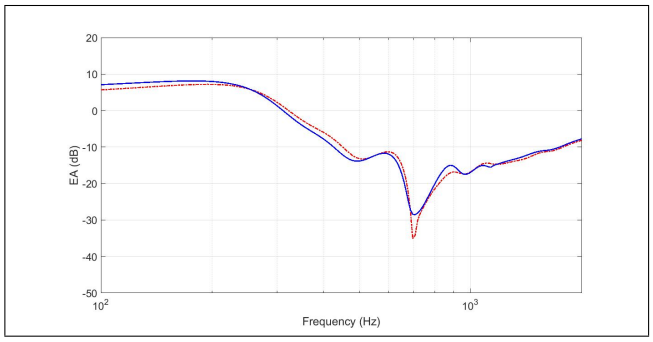

Figure 7. Three rectangular grooves per period with porous layer, d_q=[0.05,0.05,0.05], a_q=[0.04,0.04,0.04], h_q=[0.05, 0.05, 0.05], l_q=[0.15, 0.1, 0.05] (Solid=Modal (Z_{eff}), broken=BEM).

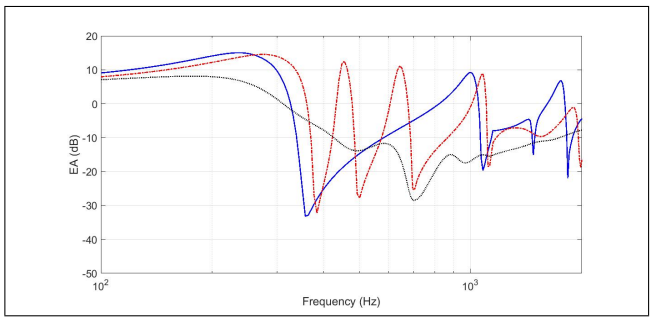

Figure 8. The modal model results overlaid. (Solid=Fig. 5, dot-dashed=Fig. 6, dot=Fig. 7).

Grooved structures incorporating a porous layer have also been successfully modelled using this method and the benefits of such hybrid structures have been reinforced. For a given multiple groove structure, incorporating a porous layer has shown to give wide band attenuation at the expense of peak attenuation at discrete frequencies.

6. REFERENCES

[1] A. Hessel, J. Schmoys, D.Y. Tseng. Bragg-angle blazing of diffraction gratings. In *Journal of the optical society of America* , Vol 65 No.4 pages 380–384, 1975.

[2] L. Kelders, J.F. Allard, W. Lauriks. Ultrasonic surface waves above rectangular-groove gratings. In *J. Acoust. Soc. Am.* , 103(5) Pt.1 pages 2730–2733, 1998.

[3] J.F. Allard, L. Kelders, W. Lauriks. Ultrasonic surface waves above a doubly periodic grating. In *J. Acoust. Soc. Am.* , 105(4) pages 2528–2531, 1999.

[4] S. Mellish, S. Taherzadeh, K. Attenborough. Approximate impedance models for point-to-point sound propagation over acoustically-hard ground containing rectangular grooves. In *J. Acoust. Soc. Am.* , 147(74) pages 74–84, 2020.

[5] J. Zhu, Y. Chen, X. Zhu, F.J. Garcia-Vidal, X. Yin, W. Zhang, X. Zhang. Acoustic rainbow trapping. In *Sci. Rep.* , 3:1728 pages 1–6, 2013.

[6] T. Wu, T.J. Cox, Y.W. Lam. From a profiled diffuser to an optimized absorber. In *J. Acoust. Soc. Am.* , 108 pages 643–650, 2000.

[7] L. Schwan, A. Geslain, V. Romero-Garcia, J.P. Groby. Complex dispersion relation of surface acoustic waves at a lossy metasurface. In *Appl. Phys. Lett.*, 110 pages 051902-1–5, 2017.

[8] R. Zhao, T. Liu, C.Y. Wen, J. Zhu, L. Cheng. Impedance-Near-Zero Acoustic Metasurface for Hypersonic Boundary-Layer Flow Stabilization. In *Phys. Rev. Appl.*, 11 pages 044015-1–5, 2019.

[9] Y.F. Zhu, X.Y. Zou, R.Q. Li, X. Jiang, J. Tu, B. Liang, J.C. Cheng. Dispersionless Manipulation of Reflected Acoustic Wavefront by Subwavelength Corrugated Surface. In *Sci. Rep.*, 5:10966 pages 1-11, 2015.

[10] Y. Zhu, X.Y. Zou, B. Liang, J.C. Cheng. Acoustic one-way open tunnel by using metasurface. In *Appl. Phys. Lett.*, 107 pages 113501-1–4, 2015.

[11] L. Schwan, O. Umnova, C. Boutin. Sound absorption and reflection from a resonant metasurface: Homogenisation model with experimental validation. In *Wave Motion.*, 72 pages 154–172, 2017.

[12] C.F. Chien, W.W. Soroka. Sound propagation along an impedance plane. In *J. Sound and Vib.*, 43(1) pages 9–20, 1975.

[13] W. Zhu, M.R. Stinson, G.A. Daigle. Scattering from impedance gratings and surface wave formation. In *J. Acoust. Soc. Am.* , 111(5) Pt.1, 2002.

[14] I. Bashir. Acoustical Exploitation of Rough, Mixed Impedance and Porous Surfaces Outdoors. In *Open University PhD Thesis*, 2013.

[15] K. Attenborough. Acoustical characteristics of porous materials. In *Phys. Rep.* , Vol 82, pages 179–227, 1982.

[16] S.I. Thomasson. A Powerful Asymptotic Solution for Sound Propagation above an Impedance Boundary. In *ACUSTICA.* , Vol 45, pages 123–125, 1980.

[17] K. Attenborough, K.M. Li, K. Horoshenkov. Predicting the acoustical properties of outdoor ground surfaces. In *Predicting Outdoor Sound*, pages 63–65, 2007.

[18] C. Zwicker, C.W. Kosten. Sound absorbing materials. *Elsevier Amsterdam*, 1949.

[19] I. Tolstoy. Smoothed boundary conditions, coherent low-frequency scatter, and boundary modes. In *J. Acoust. Soc. Am.* , 75(1), 2002.

[20] G. Kirchoff. Ueber den Einflufs der Warmeleitung in einem Gase auf die Schallbewegung. In *Ann. Phys. Chem.* , Vol 134, pages 177–193, 1868.

[21] J. Forssen (Courtesy of the Open University and HOSANNA). Toolbox from the EC FP7 HOSANNA project for the reduction of road and rail traffic noise in the outdoor environment. In *HOSANNA* , 2013.

[22] J.W. Strutt (Lord Rayleigh). On the dynamical theory of gratings. In *Proc. R. Soc, Lond.* , A 79, pages 399–416, 1907.

[23] V. Twersky. Multiple scattering of sound by correlated monolayers. In *J. Acoust. Soc. Am.* , 73, pages 68–84, 1983.

[24] J.A. DeSanto. Scattering from a perfectly reflecting arbitrary periodic surface: An exact theory. In *Radio Science* , Vol 16(6), pages 1315–1326, 1981.

[25] W. Zhu, M.R. Stinson, G.A. Daigle. Scattering from impedance gratings and surface wave formation. In *J. Acoust. Soc. Am.* , 111(5) Pt.1, pages 1996–2012, 2002.

[26] C.M. Linton, I. Thompson. Resonant effects in scattering by periodic arrays. In *Elsevier Wave Motion* , 44, pages 165–175, 2007.

[27] M.A. Biot. Theory of propagation of elastic waves in a fluid-saturated porous solid. In *J. Acoust. Soc. Am.* , Vol 28, pages 168–191, 1956.

[28] J.L. Uretsky. Scattering of plane waves from periodic surfaces. In *Ann. Phys. (N.Y.)* , Vol 33, pages 400–427, 1965.

[29] P.C. Waterman. Scattering by periodic surfaces. In *J. Acoust. Soc. Am.* , Vol 57, pages 791–802, 1975.

[30] I. Bashir, S. Taherzadeh, K. Attenborough. Diffraction-assisted rough ground effect: models and data. In *J. Acoust. Soc. Am.* , 133, pages 1281–1292, 2013.

[31] D. Berry, S. Taherzadeh and K. Attenborough. Acoustic Surface Wave Generation over Rigid Cylinder Arrays on a Rigid Plane. In *J. Acoust. Soc. Am.* , 146(4), pages 2137–2144, 2019.

[32] C.M. Linton, P.A. Martin. Multiple scattering by random configurations of circular cylinders: second-order corrections for the effective wave number. In *J. Acoust. Soc. Am.* , 117, pages 3413–3423, 2005.